BAIKAL-GVD

Deep underwater muon and neutrino detector on Lake Baikal (Gigaton Volume Detector)

JINR Group

I. Belolaptikov, V. Brudanin, V. Belov, R. Dvornitsky, Y. Hons, Z. Hons, M. Fomina, A. Klimenko, K. Konischev, A. Kuznetsov, L. Perevozschikov, E. Pliskovskiy, S. Vasilev, A. Smagina, B. Shaibonov, E. Shevchik

Team leaders: I.Belolaptikov, V.Brudanin

Dubna 2014

Introduction

The BAIKAL-GVD Project in the Lake Baikal [1] is an extension of the research and development work performed over the past several years by the BAIKAL Collaboration on the first phase. The optical properties of the deep-water lake have been established [2], and the detection of high-energy neutrinos has been demonstrated with the existing detector NT200/NT200+[3, 4]. This achievement represents a proof of concept for commissioning a new instrument, the Gigaton Volume Detector (BAIKAL-GVD), with superior detector performance and an effective telescope size at or above the kilometer-scale.

The second-stage neutrino telescope BAIKAL-GVD will be a new research infrastructure aimed primarily at studying astrophysical neutrino fluxes. The detector will utilize Lake Baikal water instrumented at depth with optical sensors that detect the Cherenkov radiation from secondary particles produced in interactions of high-energy neutrinos inside or near the instrumented volume. The concept of BAIKAL-GVD is based on a number of evident requirements to the design and architecture of the recording system of the new array: the utmost use of the advantages of array deployment from the ice cover of Lake Baikal, the extendibility of the facility and provision of its effective operation even in the first stage of deployment, and the possibility of implementing different versions of arrangement and spatial distribution of light sensors within the same measuring system.

The next generation neutrino telescope, BAIKAL-GVD, will be aimed primarily at studying astrophysical neutrino fluxes and, in particular, mapping the high-energy neutrino sky in the Southern Hemisphere including the region of the galactic center. Other topics include indirect search for dark matter by detecting neutrinos produced in WIMP annihilation in the Sun or in the center of the Earth. BAIKAL-GVD will also search for exotic particles like magnetic monopoles, super-symmetric Q-balls or nuclearites.

The detector will utilize Lake Baikal water instrumented at depth with light sensors that detect the Cherenkov radiation from secondary particles produced in interactions of high-energy neutrinos inside or near the instrumented water volume. The site chosen for the experiment is in the southern basin of Lake Baikal. Here combination of hydrological, hydrophysical, and landscape factors is optimal for deployment and operation of the neutrino telescope. Lake depth is about 1360 m here at distances beginning from about of three kilometers from the shore. The flat lake bed throughout several tens of kilometers from the shore allows practically unlimited instrumented water volume for deep underwater Cherenkov detector. A strong up to 1 m thick ice cover from February to the middle of April allows telescope deployment, as well as maintenance and research works directly from the ice surface, using it like a solid and fixed assembling platform. The light propagation in the Baikal water characterized by an absorption length of about 20-25 m and a scattering length of 30-50 m. The water luminescence is moderate at the detector site. The first generation Baikal Neutrino Telescope NT200 is operating in Lake Baikal since April 1998 [5, 6, 7]. The upgraded Baikal telescope NT200+ was commissioned in April, 2005, and consists of central part (the former, densely instrumented NT200 telescope) and three additional external strings. The deployment of the NT200+ was a first step towards a km^3-scale neutrino telescope in Lake Baikal. The first prototype of the GVD electronics was installed in Lake Baikal in April 2008 [8]. It was reduced-size section with 6 optical modules (OMs). This detection unit provided the possibility to study basic elements of the future detector: new optical modules and Flash Analog-to-Digital Converter (FADC) based measuring system. During the next two years different versions of prototype string were tested in Lake Baikal as a part of the NT200+ detector. The 2009 prototype string consists of 12 optical modules with six photomultiplier tubes (PMTs) R8055 and six XP1807 [9, 10]. In April 2010, the string with 8 PMTs R7081HQE and 4 PMTs R8055 was deployed in Lake Baikal. The operation of these prototype strings in 2009 and 2010 allows first assessment of the DAQ performance [11, 12, 13].

Specific Project Objectives

Neutrinos from local astrophysical objects

The natural high-energy neutrino fluxes are produced by physical processes in astro-physical objects characterized by enormous energy release at rates from 10^{39} to 10^{52} erg/s or higher. The nearest (with respect to a terrestrial observer) astrophysical objects that are currently assumed to be capable of emitting high-intensity neutrino fluxes are located mainly in the vicinity of the Galactic center and in the Galactic plane. Supernova remnants, pulsars, the neighborhood of the black hole Sgr A* at the Galactic center, binary systems containing a black hole or a neutron star, and clusters of molecular clouds that are targets for cosmic-ray protons and nuclei are the most promising Galactic sources with respect tothe detection of their neutrino emission. The energy spectrum of neutrinos from Galactic sources fills the energy range $10^3 \div 10^6$ GeV.

Extragalactic objects — active galactic nuclei (AGN), gamma-ray bursts (GRB), starburst galaxies and galaxy clusters — belong to another class of neutrino sources whose emission can be recorded by ground-based facilities. This class of sources is characterized by much greater energy release and generates neutrinos in the energy range $10^4 \div 10^8$ GeV or higher. Searching for a neutrino signal from identified sources imposes stringent requirements on the resolution of neutrino telescopes from the viewpoint of measuring both neutrino energy and direction.

Diffuse neutrino flux

The other direction of research on the astrophysical neutrinos is to investigate the energy spectrum, global anisotropy, and neutrino flavor composition of the diffuse neutrino flux from unidentified sources at energies above 10^4 GeV, at which the background from atmospheric neutrinos is comparable to or lower than the expected flux. The diffuse high- energy neutrino flux near the Earth is produced by neutrino emission from the entire set of sources during the period from remote cosmological epochs to the present day. Extragalactic sources make a major contribution to this flux. The neutrinos produced by the interaction of cosmic rays with interstellar matter and, in the case of ultra-high-energy cosmic rays, with electromagnetic radiation from a wide energy range, including the cosmic microwave background, also contribute to the diffuse flux. It should be noted that the neutrinos from the decay of supermassive particles associated, in particular, with Grand Unified Theories (GUT) (top-down scenario) could account for a certain fraction of the diffuse flux.

The standard approach used by a wide range of theoretical models describing the formation of neutrino fluxes in cosmic-ray sources suggests the production of neutrinos mainly during the decay of π-mesons produced in *pp* and *pγ* interactions. In this case, the flavor ratio of emitted neutrino flux is approximately $\nu_e : \nu_\mu : \nu_\tau \approx 1 : 2 : 0$. This ratio changes withdistance to the source due to the neutrino oscillations. According to Super-Kamiokande experimental data [**14**], the $\nu_\mu - \nu_\tau$ oscillation length when choosing the oscillation parameters $\delta m^2 = 2.5 \times 10^{-3}$ eV^2 and sin2θ=1 is about of $L_{osc} \sim 1.3 \times 10^{-4} (E_\nu / 1 \text{ PeV})$ parsecs.Thus, the oscillation length turns out to be much smaller than the characteristic distances to the presumed astrophysical sources of high-energy neutrinos and the flavor ration is transformed in $\nu_e : \nu_\mu : \nu_\tau \approx 1 : 1 : 1$.

Dark matter

One of the challenges of modern natural science is to find dark matter particles. Observational data in the field of astronomy and cosmology irrefutably suggest that, apart from ordinary matter, there is matter of a new type - dark matter - in galaxies, galaxy clusters, and the Universe as a whole. Moreover, on the whole, the mass of dark matter in the Universe exceeds that of ordinary matter by a factor of 5-6.

To all appearances, dark matter is composed of as yet unknown particles with the masses which exceed appreciably that of the heaviest known stable elementary particle - the proton. These new particles must have a lifetime comparable to or exceeding the age of the Universe. Undoubtedly, such a long lifetime is related to new conservation laws in fundamental physics. It can be said with great confidence that a whole stratum of new phenomena in particle physics occurring at ultra-high energies and inaccessible to investigation on existing accelerators stands behind the dark matter particles.

Dark matter particles would interact very weakly with ordinary matter. Therefore, their direct detection, if at all possible, is an extremely complicated problem of experimental physics. An indirect approach to detect dark matter particles associated with the search for the products of their annihilation at the center of the Earth, the Sun, or the Galaxy is also very promising. There must be neutrinos of fairly high energies among these products, which, in turn, interact very weakly with matter and pass through the Earth or the Sun virtually without absorption. Neutrinos of such energies are successfully recorded on large underground facilities and neutrino telescopes placed in natural media.

The methods of searching for dark matter particles with underground detectors and neutrino telescopes in natural media consist in recording an excess of the muon flux in a direction away from the center of the Earth or the Sun or from the Galactic center above the background from atmospheric neutrinos. The constraints on the additional muon flux in a direction away from the Earth's center and the Sun have been obtained on the Baksan, Super-Kamiokande, and MACRO underground facilities as well as on the underwater and under-ice neutrino telescopes NT200 (Lake Baikal), ANTARES (Mediterranean Sea), AMANDA and IceCube (South Pole). Underground neutrino detectors have a lower muon detection energy threshold (~ 1÷3 GeV) than deep underwater (under-ice) facilities. Therefore, these two classes of detectors complement each other. The former are efficient at searching for particles with a mass below 80 GeV (the threshold *W*-boson production energy), while the latter are efficient at investigating particles with a mass of about 100 GeV or higher.

A further substantial increase in the sensitivity of an experiment to the muon flux from the annihilation of dark matter particles can be achieved only by increasing their effective area. In the case of neutrino telescopes, the problem is reduced to creating cubic-kilometer facilities. In the case of underground facilities, such an increase in the effective area implies an increase in the characteristic detector sizes to a hundred meters or more. Creating such a huge underground facility seems extremely unrealistic at present.

Atmospheric neutrinos

Cosmic rays generate the most intense neutrino flux observed in ground-based experiments in the energy range from hundreds of MeV to hundreds of TeV. A large number of pions and kaons are produced when cosmic rays interact with atmospheric matter. The pion, kaon, and muon decay reactions

$$\pi^{\pm} \rightarrow \mu + \nu_{\mu};\ \ K^{\pm} \rightarrow \mu + \nu_{\mu};\ \ \mu \rightarrow e + \nu_{\mu} + \bar{\nu}_e$$

produce the neutrinos which are referred to as *conventional* atmospheric neutrinos. In the energy range 100 GeV÷100 TeV, the spectrum of *conventional* atmospheric neutrinos is described by the expression:

$$\frac{d^2N}{dE_{\nu}d\Omega}(E_{\nu},\theta) = A_{\nu}(E_{\nu}/\text{ГэВ})^{-\gamma}\left[\frac{1}{1+6E_{\nu}/E_{\pi}(\theta)} + \frac{0.213}{1+1.44E_{\nu}/E_K(\theta)}\right],$$

where A_{ν} = 0.0285 GeV^{-1} cm^{-2} s^{-1} ster^{-1}, γ = 2.69, E_{π} and E_K are the critical energies of the pions and kaons (the energies at which the decay probability is equal to the interaction probability) dependent on the zenith angle θ.

The primary cosmic rays are distributed isotropically near the Earth, but the development of cascades initiated by primary radiation in the atmosphere breaks the isotropy of the fluxes of secondary particles. The pions and kaons produced by a primary particle at large zenith angles spend much of their time in a rarefied atmosphere, where the decay probability is higher than the interaction probability. Therefore, the horizontal neutrino flux exceeds the vertical one. As the energy grows, the lifetime of pions and kaons increases and, accordingly, the decay probability decreases compared to the interaction probability. Therefore, the energy spectrum of the neutrinos produced by pions and kaons becomes steeper with growing energy (the exponent γ increases by one) than the primary cosmic- ray spectrum. The uncertainty in the predictions of the neutrino fluxes from pions and kaons is related to the uncertainty in the cosmic-ray flux and energy spectrum as well as to the uncertainty in the fraction of the kaons and pions produced in a nuclear interaction at high energies. The difference in the spectra of atmospheric neutrinos from pions and kaons calculated by different authors is about 25%.

A different neutrino production mechanism is possible at energies above 100 TeV. The *prompt* neutrinos can be produced in the decays of charmed mesons and baryons with a lifetime of the order of or less than 10^{-12} s. The spectrum of prompt neutrinos essentially follows the cosmic-ray spectrum and is flatter than that of conventional neutrinos. No prompt neutrinos have been experimentally detected so far. According to calculations, the energy at which the fluxes of prompt neutrinos become equal to and then exceed the conventional neutrino fluxes depends on the model for the interaction of primary cosmic rays with the air nuclei and on the zenith angle. For the vertical neutrino flux, this energy lies within the range 100-1000 TeV and increases with zenith angle.

From the viewpoint of experiments on neutrino telescopes, atmospheric neutrinos are the source of the natural irreducible background that complicates significantly the detection of astrophysical neutrinos. On the other hand, since the theoretical prediction level of the intensity and characteristics of the atmospheric neutrino flux is fairly high, this flux can be effectively used as a calibration neutrino flux. In addition, searching for prompt neutrinos is an important scientific task.

Magnetic monopoles

The concept of a magnetic monopole was introduced into the modern physical theory in 1931 by Dirac [15]. He showed that any magnetic charge should be a multiple of the minimum possible charge g uniquely related to the minimum electric charge:

$$g = (\hbar c/2e) \approx (137/2e).$$

Thus, the minimum magnetic charge is approximately a factor of 68.5 larger than the minimum electric charge. In particular, this implies that the ionization energy losses for relativistic monopoles in a medium are much larger than those for relativistic muons. This opens good possibilities for the detection of fast monopoles in experiments with neutrino telescopes. The theory of Cherenkov radiation from magnetic monopoles was first examined by I.M. Frank [16]. The linear density of Cherenkov radiation with a wavelength A (under the assumption that the permeability of the medium is μ ~ 1) is described by the expression

$$\frac{d^2 n_c}{dx d\lambda} = \frac{2\pi\alpha}{\lambda^2}\left(\frac{ng}{e}\right)^2\left(1 - \frac{1}{n^2\beta^2}\right),$$

where g is the magnetic charge of the monopole, e is the charge of electron, n is the refractive index of the medium (for water, n = 1.33), $\beta = \upsilon/c$ is a monopole velocity expressed in units of the speed of light in vacuum and a is the fine-structure constant.

The Cherenkov radiation from a relativistic monopole in water is a factor of $(ng/e)^2 \approx 8300$ more intense than that from a relativistic muon. Thus, a magnetic monopole with a speed β ~ 1 is a bright light source corresponding in intensity to a muon with an energy of ~ 1.4 x 10^4 TeV. Intense searches for magnetic monopoles stimulated by the works [17, 18] have been performed since the mid-1970s. In these works, it was shown for the first time that the possibility of the existence of topological defects in the form of magnetic monopoles in the Universe is a corollary of Grand Unified Theories (GUT). The masses of these particles lie in a wide range from ~ 10^8 GeV to ~ 10^{21} GeV, depending on the GUT versions. The most reliable astrophysical constraints on the natural flux of monopoles are: the Chudakov-Parker limit [19-21] derived from the condition for the conservation of the observed Galactic magnetic field strength

and the *cosmological* constraint following from the obvious condition

$$F_{\rm mon} < 10^{-15}\text{cm}^{-2}\text{s}^{-1}\text{ster}^{-1},$$

which yields

$$F_{\rm mon} < 1.4 \cdot 10^{-12}\beta[(10^{16}\text{GeV}/c^2)/m_{\rm mon}]\text{cm}^{-2} \cdot \text{sec}^{-1} \cdot \text{ster}^{-1} \ .$$

Both these constraints do not rule out the possibility of a local excess above these limiting fluxes of monopoles, for example, in the Solar system. As a result of its acceleration in Galactic magnetic fields, the kinetic energy of a heavy monopole can reach ~ 10^{11} GeV. On the other hand, when passing through the Earth, the energy losses of quasi-relativistic monopoles with $\beta>\beta_c$ (β_c = 0.75 is the threshold speed of the monopole with respect to the generation of Cherenkov radiation) are ~ 10^{11} GeV. It thus follows that monopoles with a mass of less than 10^{11} GeV passing through the Earth remain quasi-relativistic and can be detected by their Cherenkov radiation with neutrino telescopes.

In 1981, V. Rubakov [22] published a paper where he concluded that the processes with baryon number nonconservation are not suppressed in the presence of a monopole predicted by Grand Unified Theories. A similar conclusion was reached in 1982 by Callan [23]. The cross section for the reaction of monopole catalysis of baryon decay was estimated as

$$\sigma_{\rm cat} = \sigma_0\beta_{\rm mon}^{-1},$$

where a_0 was taken to be equal in order of magnitude to the characteristic values of strong interactions: a_0 ~ 10^{-28} cm^2. When the electromagnetic interaction between a monopole and a nucleus incorporating a nucleon is taken into account, the factors $F(\beta_{mon})$ = 2.4 • $10^7\beta_{\rm mon}{}^{3.1}$for the nucleons constituting the ^{16}O nucleus and $F(\beta_{\rm mon}) = 0.17 \cdot \beta_{\rm mon}^{-1}$for freeprotons appear in the expression for the catalysis cross section. A monopole moving in water with a speed less than or of the order of 10^{-3} of speed of light must initiate mainly the decay of hydrogen nuclei with the cross section

$$\sigma_{\rm cat}^p = 0.17\sigma_0\beta_{\rm mon}^{-2}.$$

The energy being released in a single catalysis event (m_pc^2 = 938 MeV) is distributed between the proton decay products. While propagating in water, the latter become the sources of Cherenkov radiation, which is also generated by their daughter particles, δ-electrons, e^+e^-pairs, etc. As a result of each proton decay, up to N_γ = 1.1 • 10^5 Cherenkov photons are emitted in the wavelength range 300 <λ< 600 nm. Thus, the trajectory of the muon inducing proton decays when crossing a water volume must appear as a chain of flashes with a Cherenkov spectrum. If the decays occur frequently, for example, 10 —10^3 per 1 cm of the monopole path, then the detection rate of Cherenkov photons emitted by decay products can noticeably exceed the pulse count rate attributable to the photomultiplier dark current and water luminescence. The method of searching for slow monopoles in experiments on neutrino telescopes is based on the selection of such events [24].

Neutrino Interactions

Natural high-energy neutrinos interact with the target material of neutrino telescopes mainly through the reactions on nucleons via the channels of charged (CC) and neutral (NC) currents:

$$\nu_l(\bar{\nu}_l) + N \overset{\text{CC}}{\rightarrow} l^-(l^+) + \text{hadrons}, \tag{3.1}$$
$$\nu_l(\bar{\nu}_l) + N \overset{\text{NC}}{\rightarrow} \nu_l(\bar{\nu}_l) + \text{hadrons}, \tag{3.2}$$

where l = e, n or τ. The interaction of neutrinos with target electrons makes virtually no contribution to the total number of recorded events, except for the resonant scattering of electron antineutrinos in the W-resonance region:

$$\bar{\nu}_e + e^- \rightarrow W^- \rightarrow \text{anything}, \tag{3.3}$$

with the energy at resonance $E_0 = M_W^2/2m_e = 6.3 \times 10^6$ GeV and a cross section of 5.02 x 10^{-31} cm^2. The final products of reactions (3.1)-(3.3) — leptons and high-energy cascades — carry information about the energy, direction, and, in principle, flavor of neutrinos.

In experiments on deep underwater and under-ice Cherenkov detectors, the effective target size depends on the neutrino energy and flavor. In the case of muon neutrinos, both the transparent medium around the telescope and the bedrock are the neutrino target, because the secondary muons have a high penetrating power. In the former case, the muon neutrino energy can be determined by reconstructing the energies of the muon and the shower generated at the neutrino interaction vertex. During a muon neutrino interaction in rock, the neutrino energy in each individual event cannot be reconstructed exactly due to the energy losses of the muon as it propagates from the interaction vertex to the facility. However, when the statistics of recorded events is large enough, the energy spectrum of the muon neutrino flux can be derived by the reconstruction of the muon energy. The astrophysical fluxes of ν_e and ν_τ, which account for two thirds of the total flux, can be investigated in experiments on neutrino telescopes only by recording the secondary showers generated in a water target. Hadronic showers are produced in the interactions of neutrinos of all flavors with nuclei via the channels of charged and neutral currents. In addition, in the case of the CC interaction of electron and τ-neutrinos, the electron energy is converted into the energy of an electromagnetic shower, while a significant fraction of the τ-lepton energy is transferred to the hadronic or electromagnetic shower as a result of its decay. Thus, achieving a high accuracy of reconstructing the energy and direction of showers is an indispensable requirement for efficient detection of neutrinos of all flavors.

Basic Methods and Approaches Used in the Project

The astrophysical neutrino fluxes are investigated with neutrino telescopes in two main directions of research [25-27]. The first direction of research is concerned with the search for a neutrino signal from known astrophysical objects or the detection of unidentified local sources from observations of the signal excess above the background level over the entire celestial sphere. Figure 1sketches the two basic detection modes of underwater neutrino telescopes. CC muon neutrino interactions produce a muon track (left), whereasother

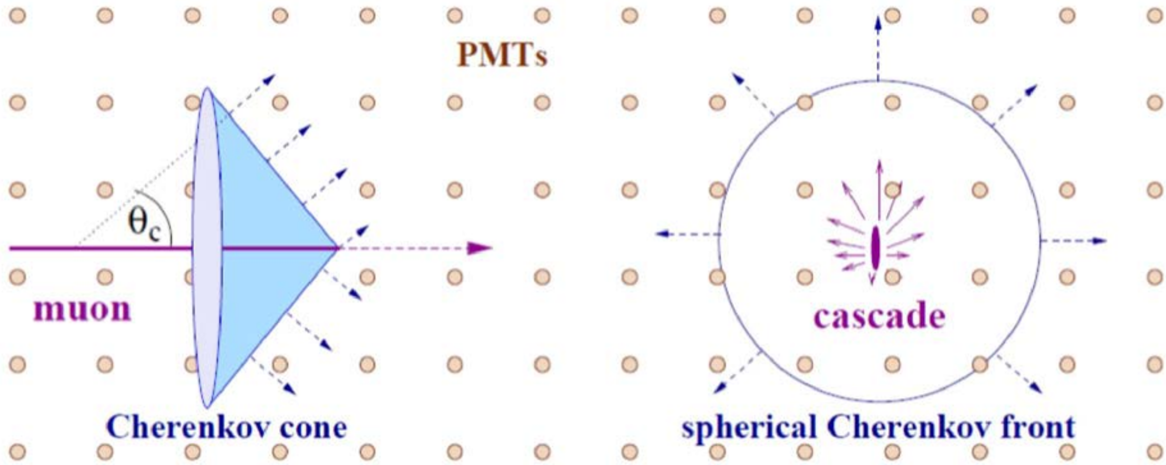

Figure 1: Detection principles for muon tracks (left) and cascades (right) in underwater detectors. Note that the Cherenkov light emission by cascades is peaked at the Cherenkov angle θ_c with respect to the cascade axis but has a wide distribution covering the full solid angle.

neutrino reaction types cause hadronic and/or electromagnetic cascades (right). This is, in particular, true for NC reactions (hadronic cascade) or CC reactions of electron neutrinos (overlapping hadronic and electromagnetic cascades). CC tau neutrino interactions can have either signature, depending on the τdecay mode.

The BAIKAL-GVD is 3 dimensional lattice of photomultiplier tubes each enclosed in a transparent pressure sphere to comprise an optical module. The OMs are arranged on vertical load-carrying cables to form strings. The configuration of telescope consists of clusters of strings - functionally independent sub arrays, which are connected to shore by individual electro-optical cables (see figure 2). Each cluster comprises eight strings of optical modules - seven peripheral strings are uniformly arranged at a 60 m distance around a central one. Optical modules are spaced by 15 m along each string and are faced downward. OMs on each string are combined in sections - detection units of telescope. The distances between the central strings of neighboring clusters are H=300 m.

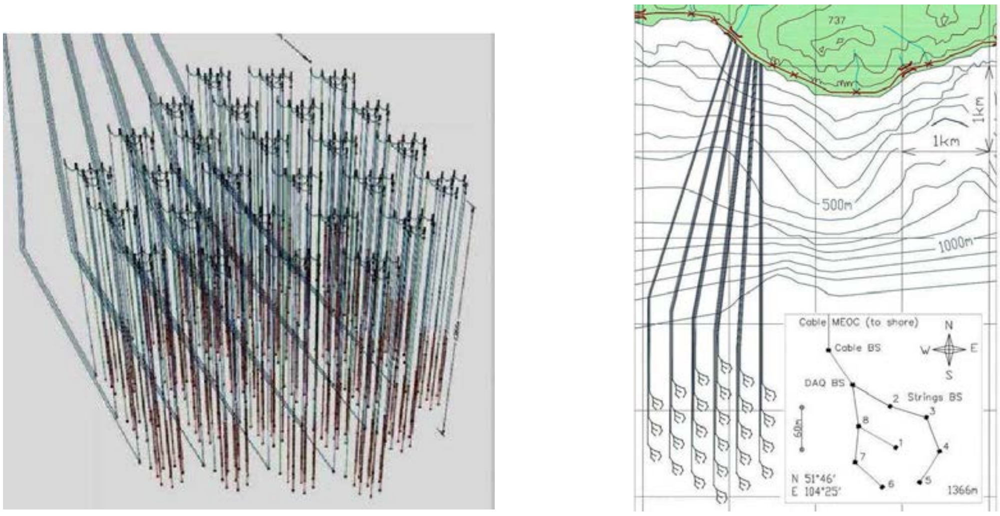

Figure 2: Left: Artistic view of the GVD-telescope. Right: Layout of the GVD. In inner box layout of the GVD-cluster is shown.

The objective of the optimization of the BAIKAL-GVD design was to provide a large cascade detection volume with the requirement of effectively recording high energy muons. Muon effective areas for two optimized BAIKAL-GVD configurations are shown in Fig. 3(left). The curves labeled by GVD*4 and BAIKAL-GVD relate to configurations with 10368 OMs and 2304 OMs, respectively. Muon effective area (6/3 condition — at least 6 hit channels on at least 3

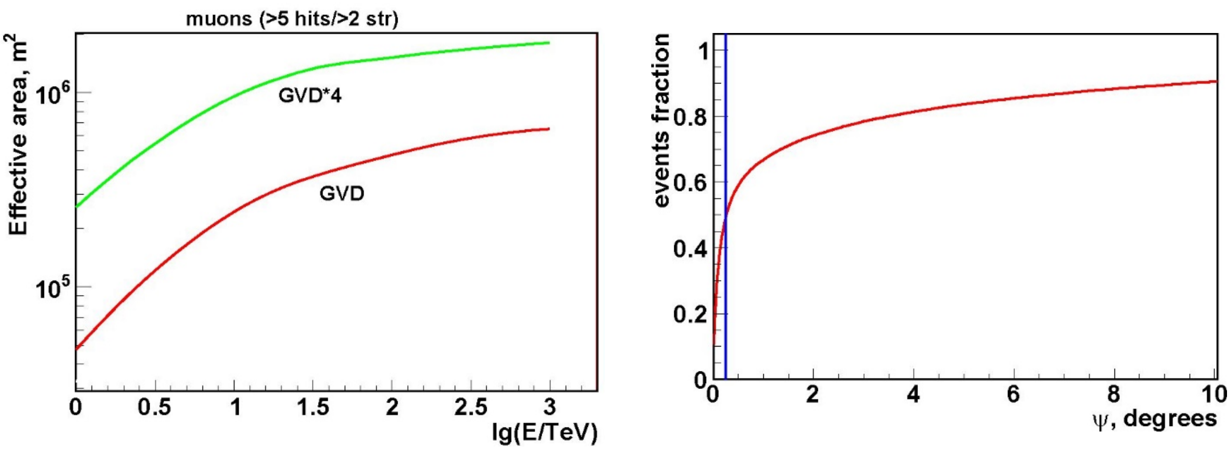

Figure 3: Left: Muon effective area. The curves labeled by GVD*4 and GVD relate to configurations with 10368 OMs and 2304 OMs, respectively. Right: The fraction of muon events (E_{μ}> 1 TeV) with mismatch angle ψ less than a given value.

strings) rises from 0.3 km^2 at 1 TeV to 1.8 km^2 asymptotically. The fraction of events with mismatch angle between generated and reconstructed muon directions less than a given value ψ is shown in Fig. 3(right). Muon arrival direction resolution (median mismatch angle) is about of 0.25 degree.

Shower effective volumes for two BAIKAL-GVD configurations are shown in Fig. 4 (left). Shower effective volumes (11/3 condition — at least 11 hit channels on at least 3 strings) for basic configuration are about of 0.4-2.4 km^3 above 10 TeV. The accuracy of shower energy reconstruction is about of 20-35% depending on shower energy. The accuracy of a shower direction reconstruction is about 3.5-6.5 degrees (median value). Distribution of the mismatch angle between generated and reconstructed 1 PeV shower directions is shown in Fig. 4(right).

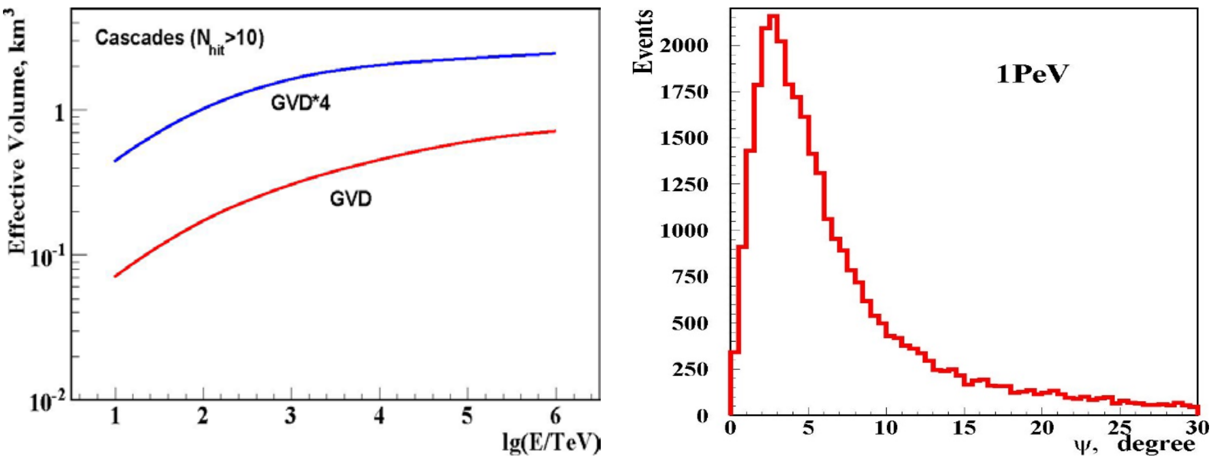

Figure 4: Left: Effective volume of cascades detection. The curves labeled by GVD*4 and GVD relate to configurations with 10368 OMs and 2304 OMs, respectively. Right: Distribution of the mismatch angle 0 between generated and reconstructed 1 PeV shower directions.

Reconstruction

The reconstruction procedure for a muon track consists of several consecutive steps which are typically:

- Rejection of noise hits;
- Simple pre-fit procedures providing a first-guess estimate for the following iterative maximum-likelihood reconstruction;
- Maximum-likelihood reconstruction;
- Quality cuts in order to reduce background contaminations and to enrich the sample with signal events. This step is strongly dependent on details of the actual analysis diffuse fluxes at high energies, searches for steady point sources, searches for transient sources etc.

An infinitely long muon track can be described by an arbitrary point $\mathbf{r_0}$ on the track which is passed by the muon at time t_0, with a direction $\mathbf{p}$ and energy E_0. Photons emitted under the Cherenkov angle ϑ_c and propagating on a straight path are expected to arrive at PMT i located at $\mathbf{r}_i$ at a time

$$t_{\text{geo}} = t_0 + \frac{\mathbf{p} \cdot (\mathbf{r_i} - \mathbf{r}_0) + d \cdot \tan\theta_c}{c},$$

$$t_{\text{res}} = t_{\text{hit}} - t_{\text{geo}}.$$

where d is the closest distance between PMT i and the track, and c the vacuum speed of light. The time residual t_{res} is given by the difference between the measured hit time and the hit time expected for a direct photon, t_{geo}:

An unavoidable symmetric contribution around Δ_t = 0 in the range of a nanosecond comes from the PMT/electronics time jitter, σ_t. Electromagnetic and hadronic cascades along thetrack lead to a tail towards larger (and only larger) time residuals. Scattering of photons can lead to an even stronger delay of the arrival time. These residuals must be properly implemented in the probability density function for the arrival times used in the maximum-likelihood procedure.

The simplest likelihood function is based exclusively on the measured arrival times. It is the product of all N_{hit} probability density functions p_i to observe, for a given value of track parameters {a}, photons at times t_i at the location of the PMTs hit:

$$L_{\text{time}} = \prod_{i=1}^{N_{\text{hit}}} p(t_{\text{res},i} \mid \{a\}).$$

More complicated likelihood functions include the probability of PMTs hit to be hit and of non-hit PMTs not to be hit, or of the respective amplitudes. Instead of referring only to the arrival time of the first photon for a given track hypothesis and the amplitude for a given energy hypothesis, one may also refer to the full waveform from multiple photons hitting the PMT. For efficient background suppression, the likelihood may also incorporate information about the zenith angular dependence of background and signal (Bayesian probability). The reconstruction procedure finds the best track hypothesis by maximizing the likelihood.

Detector Description

The detector will utilize Lake Baikal water instrumented at depth with light sensors that detect the Cherenkov radiation from secondary particles produced in interactions of high-energy neutrinos inside or near the instrumented water volume. Signal events consist of up-going muons produced in neutrino interactions in the bedrock or the water, as well as of electromagnetic and hadronic showers (cascades) from CC-interactions of ν_e and $\nu_\tau$or NC-interactions of all flavors inside the array detection volume. Background events are mainly downward-going muons from cosmic ray interactions in the atmosphere above the detector.

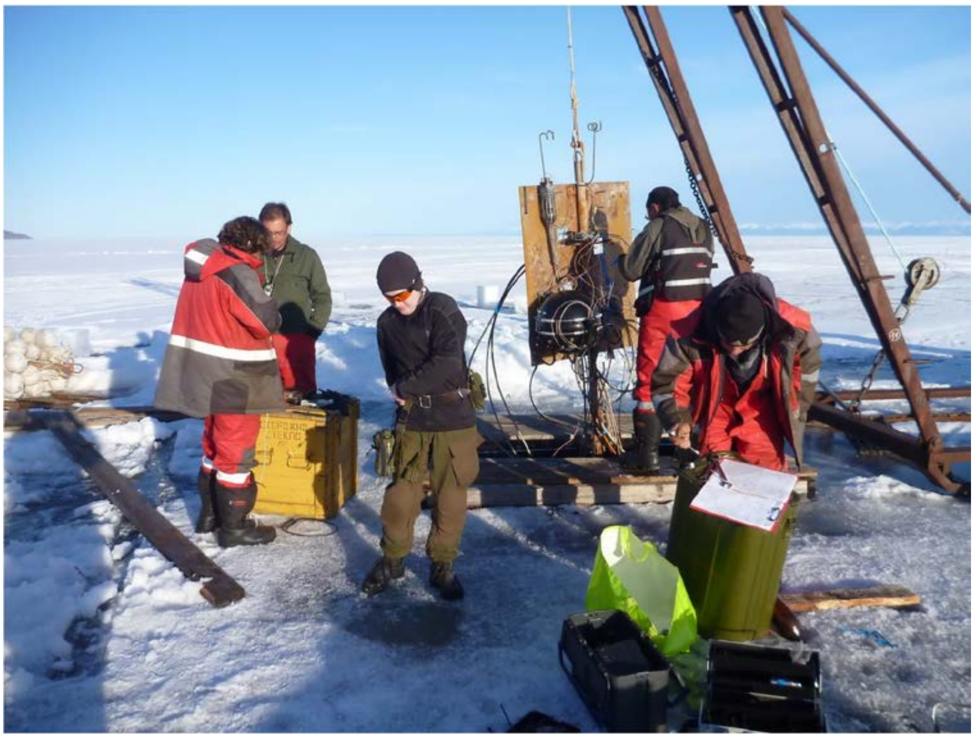

Figure 5: Installation of the demonstration cluster “Dubna”.

The concept of BAIKAL-GVD is based on a number of evident requirements to the design and architecture of the recording system of the new array: the utmost use of the advantages of array deployment from the ice cover of Lake Baikal as can be seen from Fig. 5, the extendibility of the facility and provision of its effective operation even in the first stage of deployment, and the possibility of implementing different versions of arrangement and spatial distribution of light detectors within the same measuring system.

With all above requirements taken into account, the following conceptual design of BAIKAL-GVD has been developed. The Data Acquisition System of BAIKAL-GVD is formed from three basic building blocks: optical modules, sections of OMs and clusters of strings. The OM consists of a photomultiplier tube (PMT) with large hemispherical photocathode and attendant electronics, which are placed in pressure-resistant glass sphere. The OMs are arranged on vertical load-carrying cables to form strings. Optical modules of each string are grouped into two, three or four sections. A section is a basic detection unit (DU) of array. Each section consists of 12-16 OMs and the central module (CM). PMT signals from all OMs of a section are transmitted to the CM, where they are digitized by ADC boards. The CM consists of ADC boards, an OM slow-control unit, and a Master board. The digitized signals from each ADC are transferred to a FPGA which handles the data. A memory buffer allows for accumulating the waveform data from the ADC. An ADC trigger request channel includes a request builder, which forms the request signals to the trigger logic, which are transferred to the Master board. The Master board provides trigger logic, data readout from ADC boards, connection via local Ethernet to the cluster DAQ center, and control of the section operation. The request analyzer forms the section trigger request (local trigger) on the basis of requests from ADC channels. The section trigger request is transferred to the cluster DAQ center.

The cluster DAQ center is placed near the water surface. It provides the string triggering, power supply control, and communication to shore. The organizations of central and section trigger systems are the same. The section local triggers come to inputs of the central ADC board. The central Master board works out the global trigger for all sections. The global trigger produces the stop signal for all ADC channels and initiates waveform information readout. Waveform information is accumulated in the event buffer and then transmitted via an Ethernet connection to the cluster DAQ center. The cluster DAQ center is connected to shore station by an about 6 km long electro-optical cable.

Each BAIKAL-GVD cluster is a functionally complete and independent sub-array, which can operate both as a part of unified configuration and autonomously. This allows for easy upgrade of the array configuration, as well as putting into operation its individual parts within the telescope deployment phase.

Optical Module

The basic measuring units of the BAIKAL-GVD are optical modules (OMs), which are

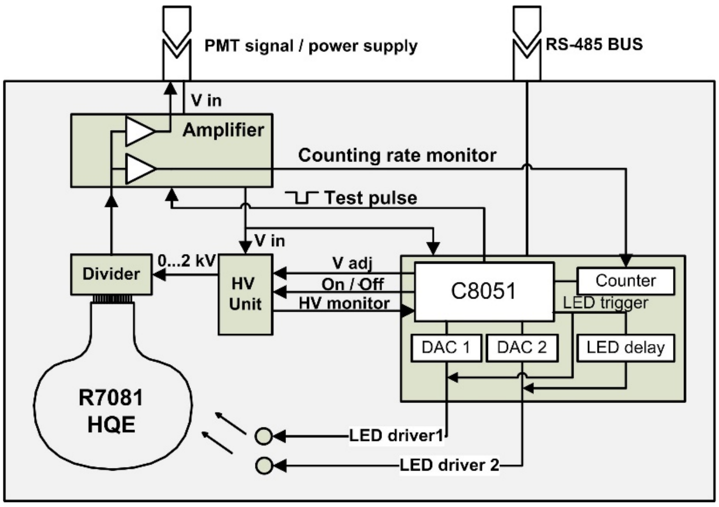

Figure 6 (a) Block diagram of optical module.

design to convert the Cherenkov radiation of muons and showers into electric signals. An OM consists of the following elements: a photo-multiplier tube (Hamamatsu-R7081HQE), a controller, an amplifier, LED calibration unit, and a high-voltage converter. The OM block scheme is shown in Fig. 6a.

Section — Detection Unit of the BAIKAL-GVD

Optical modules are mounted on vertical load-carrying cables to form strings. A low- level data collecting unit of a string is a section of optical modules. Each section contains 12 OMs, a central module (CEM), and a service module (SM). The section functional scheme is shown in Fig. 7. The central module collects and transfers data and controls the section electronics operation. Analog signals from optical modules arrive at CEM through coaxial cables 90 m long. Digitization of the PMT signal is performed in a 15-μs window by three boards of four-channel 12-bit ADC (FADC) with a discretization frequency of 200 MHz. Waveform stamps of events are formed in the channels, the analysis of which makes it possible to determine the amplitude and detection time of OM signals. Two ring buffers are

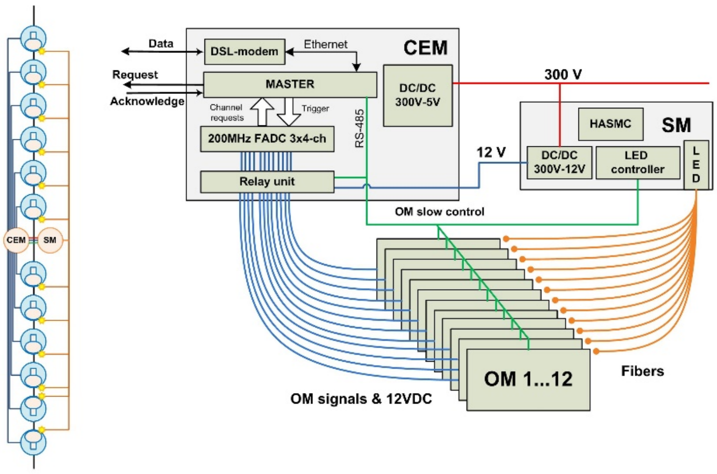

Figure 7: Functional scheme of BAIKAL-GVD section.

provided in each channel to record signal waveform with dead-time minimized. Along with the conversion of analog signals and intermediate data storage, the ADC boards form the so-called channel *request* signals. A *request* signal is formed when the input signal amplitude exceeds the specified threshold. The threshold function is implemented on digital comparators (two comparators per channel). The comparator thresholds are controlled with a step of 1.4 mV. *Request* signals from all ADC channels arrive at the *Master board,* which forms a section *request.* This signal is formed when the *request* signals from the section channels fulfill specified conditions. The information about the allowed combinations of the signals is loaded dynamically into the *Master* board memory (the so-called coincidence matrix is formed). The *request* signals of sections are transferred to the cluster center through coaxial cables 1200 m long. A *acknowledge* signal is formed in the cluster center; it serves as a global trigger for all sections and provides their synchronous operation. This signal initiates readout of the data of all ADC channels and their transfer to the data acquisition center of the cluster (DAQ-center), which is in turn connected with the shore station through an electro-optical cable.

Data from OMs of the section are read through the Ethernet channel of the *Master* board, which is elongated to 1200 m via DSL modems (transfer rate up to 8 Mbit/s). A local underwater RS-485 data bus, based on the ASCII protocol, is used for slow control (setting the modes of OM operation, calibration, and monitoring the equipment). The Ethernet to RS485 converter for slow control channel is implemented on the *Master* board. The power supply voltage is fed to optical modules from 300 V - 12 V DC/DC converters, which are mounted in the section SM. A relay control of OM switching makes it possible to switch off optical modules from the power supply unit in the case of short circuit. Along with DC/DC converters, the SM includes elements of the calibration system and the acoustic positioning system.

A section is calibrated by two pulsed LED light sources, the signals of which are branched through optical cables to all optical modules of the section. The monitoring system of the section provides information on the power supply voltage across the section and each optical module, on the temperature inside OM, on the high voltage across the photomultipliers, and on the count rate of PMT noise pulses.

String

A string is the basic structural unit of the BAIKAL-GVD detector. It is an assembly composed of several sections, positioned on the same backbone cable. The string includes two or four sections and communication module (COM). The functional scheme of a string is shown in Fig. 8.

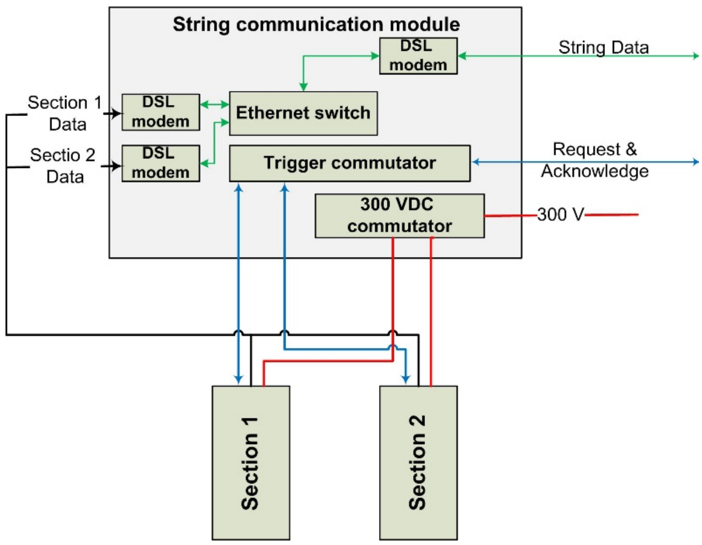

Figure 8: Functional scheme of the string communication module of BAIKAL-GVD.

The string communication module provides connection of data transfer, synchronization, and power supply systems of individual sections to the load-carrying cable, which connects the string to the cluster DAQ-center. The cable consists of two coaxial RK50 cables to translate *request* and *acknowledge* signals, three power supply wires with a cross section of 0.5 mm2 and a screened twisted pair for data transfer. The data from sections are transferred through DSL modem lines to the COM and translated (through the Ethernet switch and additional DSL modem) to the cluster DAQ-center. The *request* signals from sections are combined by a logical *OR* element in the trigger commutator unit to form the string *request* signal. The *acknowledge* signal from COM is branched to arrive at string sections. The string configuration, composed of two sections, does not need additional switching of power supply lines: each section is connected to its own power supply wire in the loadcarrying cable. The power supply voltage 300 VDC is controlled in the cluster DAQ-center through a relay commutator. The relay commutator is also planned to be used for a larger number of sections in the string communication module.

Cluster

The basic configuration of BAIKAL-GVD cluster comprises eight strings, a data acquisition center (DAQ-center), and electro-optical cable, which connects the cluster to the shore station (see Fig. 9). The DAQ-center of a cluster consists of 3 underwater modules, located at a shallow

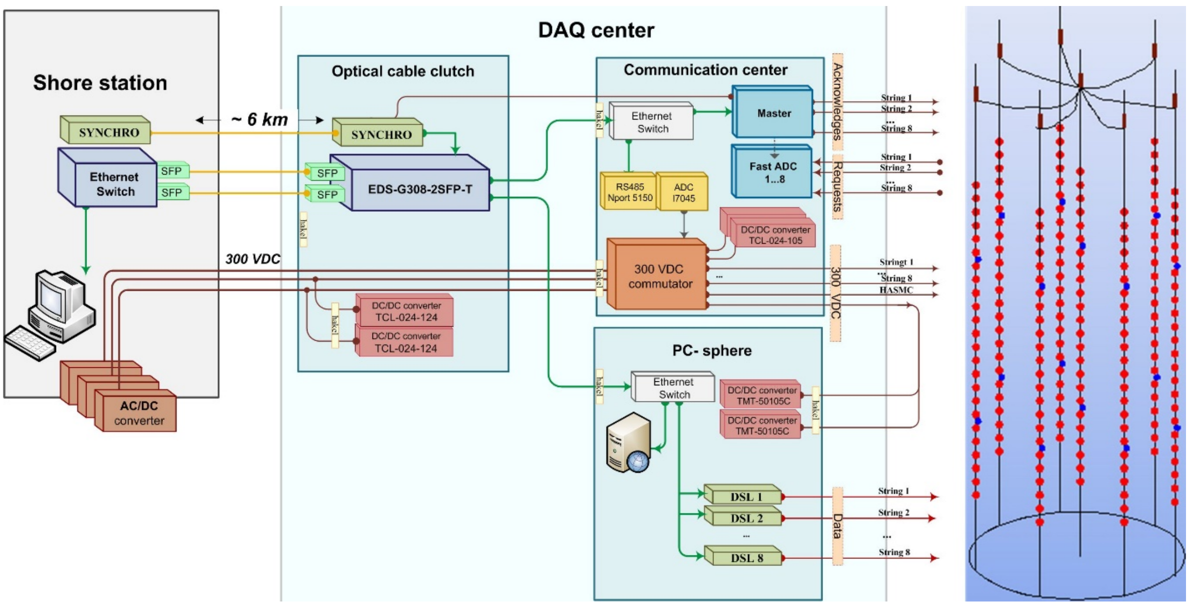

Figure 9: Functional scheme of the data acquisition center of a cluster (on the left) and a cluster composed of eight strings (on the right).

depth of about 30 m: a cluster communication center, a PC sphere, and an optical cable clutch.

Strings are connected to the DAQ-center of cluster through 1.2 km long cables, which serve to transfer data, supply power, and synchronize the operation of sections. Data from 8 strings are transferred through two-wire communication lines based on DSL modems, located in the PC-sphere (data transfer rate up to 15 Mbit/s). This module also contains an underwater microcomputer to perform on-line analysis of the information received. The string's data are transferred from the PC-sphere to the optical cable clutch through an underwater 100-Mbit Ethernet line for their subsequent translation to the shore through the Gigabit Ethernet switch EDS-G308-2SFP-T.

The cluster DAQ-center is connected to the shore by an electro-optical cable about 6 km long. This cable serves to feed the cluster and transfer digital data through a gigabit optical fiber communication line (OFCL). An OFCL consists of 3 pairs of single-mode fibers (AHWave FLEX ZWP). Two pairs are used to transfer data (main and reserve lines), and one pair is aimed at synchronizing the operation of BAIKAL-GVD clusters. Shore power supply units (AC/DC converters) with an output voltage up to 450 VDC and power up to 1 kW are used to feed a cluster. The output power supply voltage is controlled so as to provide a voltage of 300 V at the end of the 6-km underwater feed line. The underwater part of the equipment, which is designed to control the cluster power supply and to synchronize the operation of the sections, is located in the cluster communication center. Independent switching on and off the 300V power supply of each section is performed by a relay commutator, which is controlled via a 16-channel digital output module (I-7045) and RS485 serial device server (NPort 5150A-T). The relay commutator and its control devices are fed by TCL-024-124 sources, which are located in the optical cable clutch.

The operation of the measuring systems of cluster sections is synchronized by the DAQ-center *Master* and 8-channel FADC units, which are identical to the units of the section CEMs. *Request* signals from all strings arrive at the cluster DAQ-center, where their arrival times are measured. The *Master* unit analyzes the string requests and generates a *acknowledge* signal, which is branched to all sections of all strings as a global trigger. The arrival times of photons detected by section channels are measured with respect to this signal. The differences in the transit times of the *request* and *acknowledge* signals of different sections are measured with FADC units of the CEMs with an error of < 5 ns.

Trigger Formation and Data Transfer Systems

The BAIKAL-GVD data transfer and trigger systems are closely interrelated. The neutrino telescope records fairly rare events. However, to detect signal events from muons or showers by the selected trigger system at the instrumental level with a high detection efficiency, one has to reduce maximally the channel detection thresholds. As a result, background (noise) events make the main contribution to the total data flux. The background is filtered in the stage of on-line analysis of the data in the shore station. The data transfer system is aimed at transmitting the total data flow (which can be as high as several tens of Mbit/s) from the underwater part of the system to the shore station without loss.

Shore Data Acquisition and Control Center

The shore DAQ-system for collecting and processing events should be organized as follows.

Electro-optical bottom cable lines (one line per cluster) are used for power supply and data exchange of clusters. Data channels are connected to the Host PC Station through a 16- port Ethernet switch to the input of the Host Station, where the data flow is processed. The Host Station (enterprise-level server, designed, in particular, for scientific computations) is a multiprocessor platform (processors based on four or more cores) with 128-Gb RAM, in the address space of which a unified dataset is formed from the input data flow. The Host Station must have a sufficiently high reliability (up to hot replacement of components), be easy in maintenance, and flexible in distributing resources. Preliminary estimates show that this system is minimally sufficient for stable processing of the total data flow, concerning all main purposes of the system. However, in the case of unforeseen increase in the necessary computational resources of the server, the solution chosen has an advantage: its resources can easily be increased by scaling. The dataset formed is filtered, and the events that did not pass through the trigger chosen for a specific physical problem are rejected, while the events passed through the trigger are directed to the output data flow. The output data are saved either on the RAID-5 array or on external carriers. The predicted data flow from the system suggests the annual amount of the output data to be no larger than few terabytes. Thus, this configuration not only makes it possible to store data but also allows one to use, process, and transfer them on-line through the Internet. The accuracy in timing the experimental data to the world time should be better than 100 is. Such accuracy has been achieved by installing and tuning local GPS receivers and tuning the *ntp (network time protocol)* service.

The functions of the basic service program of the software system (Basic Program, BP), which is run at the Host PC, are as follows:

- Choice of the static configuration of the telescope (number of clusters, strings, addresses of data transfer controllers, etc.). Change in the dynamic parameters of the state of strings and optical modules of the telescope (setting PMT high voltages, channel thresholds, modes of the LED-flasher operation, and setting parameters in the data transfer controllers of the strings).
- Time and amplitude calibration of the detector.
- Saving the data obtained in the real-time format using a large set of information messages. The obtained data of different types are saved (after preprocessing) in data files and are indicated by corresponding marks.
- Automatic logging sessions performed and tests of measurement systems.
- Provision of an integrated set of low-level utilities that are necessary for handling separate OMs and data transfer controllers.
- Generation of monitor data (amplitude and time distributions, statistical distributions, spectra of the shape of measurement channel pulses), which is necessary for on-line monitoring the information received.

The Host PC software is developed under the Linux OS on the C and C++ languages, using Qt and ROOT graphical libraries (and the tools existing in the ROOT for developing and designing applied user interfaces). One of the key features of the shore software developed is the possibility of full remote control of the detector through specialized network protocols SSH and VNC, which are provided at the OS level. This possibility is necessary for solving current problems, maintaining the standard mode of detector operation during data collection sessions, and on-line monitoring the quality of the information received.

The use of the system for remote monitoring and controlling the detector increases significantly the efficiency of the system; however, a threat of unauthorized access to the local computational network of the telescope arises in this case. To protect the computational network from unauthorized access, it is divided into two zones: a users' zone, which contains user computers with access to the Internet, and a safety zone, with the equipment that is necessary for the telescope operation. The safety zone contains the computers of the data collection system of the telescope (Host PC); the systems for monitoring the telescope operation; and the underwater local computer network, which is connected to the shore part of the control system through a fiber cable. The local network is connected to the Internet through a router for controlling access. The router is also equipped with a firewall to exclude all unauthorized entry connections. When entering the local network, one can get access to the shore-center computers only after the corresponding authentication procedures.

Positioning System of the BAIKAL-GVD

To obtain coordinates of each OM during data taken period a custom Long-Base-Line (LBL) Underwater Acoustic Positioning System (L-UAPS) [30], developed by EvoLogics GmbH (Germany), was deployed at the detector. The system consists of a bottom LBL-antenna, comprised of nodes moored at the bottom of the telescope strings, and acoustic beacons, attached to the strings (three per string).

The measurement cycles are launched by an operator at the shore center (the minimum duration of a measurement cycle is limited to 30 s). The L-UAPS's positioning accuracy of 5 mm was experimentally proven for beacons 160 m away from the bottom antenna, thus allowing to track even the smallest movements of the drifting beacons. Measurements performed since the Cluster-2012 starts to operate. Figure 10 shows a distance monitoring between the bottom and top beacons of the string in April 2012.

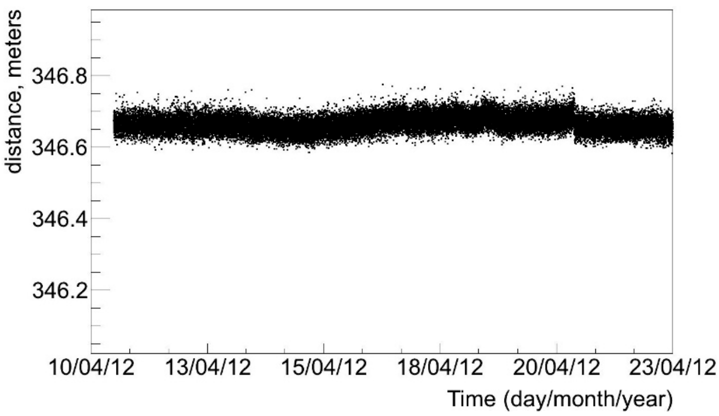

Figure 10: Measured distance between top and bottom beacons of string vs time.

Demonstration Cluster “DUBNA”

The prototyping and early construction phase of the BAIKAL-GVD project aims at in situ comprehensive tests of all elements and systems of the future telescope as the parts of engineering arrays operating in Lake Baikal.

Prototyping phase will be concluded with deployment in 2015 of the first demonstration cluster of the GVD in Lake Baikal. Demonstration cluster will comprise total of 192 optical modules arranged on eight 345 m long strings (7 side strings located at 60 m distances from a central one). Each string comprises 24 OMs spaced by 15 m at depths of 900 m to 1250 m below the surface. OMs on each string are combined in two sections. Also the demonstration cluster will comprise an acoustic positioning system and an instrumentation string with equipment for array calibration and monitoring of environment parameters. Demonstration cluster will be connected to shore by the electro-optical cable.

The potential power

Recently, the IceCube Collaboration reported on results of an all-sky search for high-energy neutrino events interacting within the IceCube neutrino detector conducted between May 2010 and May 2012 [28]. The search follows up on the previous detection of two PeV neutrino events [29], with improved sensitivity and extended energy coverage down to about 30 TeV. Twenty- six additional events were observed, substantially more than expected from atmospheric backgrounds. Combined, both searches reject a purely atmospheric origin for the 28 events at the 4.3 α level. These 28 events, which include the highest energy neutrinos ever observed, have flavors, directions, and energies inconsistent with those expected from the atmospheric muon and neutrino backgrounds. These properties are, however, consistent with generic predictions for an additional component of extraterrestrial origin with (1:1:1) flavor ratio.

In this search events were selected based on the requirement that they display a vertex (shower pattern) contained within the instrumented ice volume, effectively employing the edges of the IceCube detector as a veto for downgoing muons. The data are well described in this energy range by an E^{-2} neutrino spectrum with a per-flavor normalization of $E^2F(E)$ = (1.2±0.4) x 10^{-8} GeV cm^{-2} s^{-1} sr^{-1}.

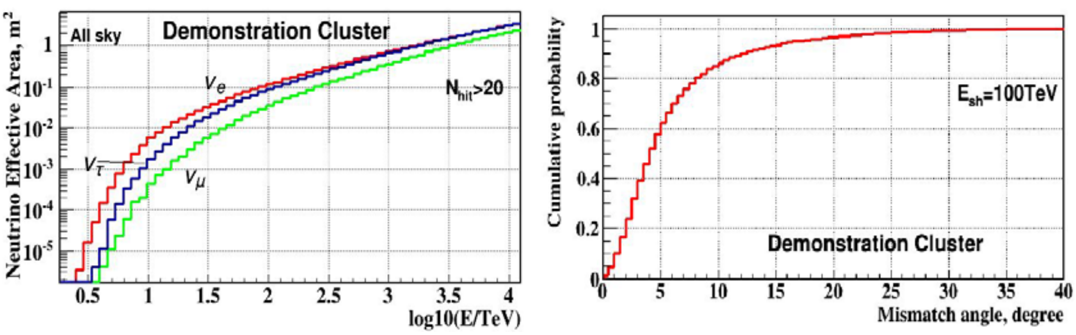

Figure 11: Left: Neutrino effective areas averaged over all arrival angles.

Baikal collaboration has a long experience on studies of muons and neutrinos by detection and reconstruction of secondary high-energy cascades. The limits on all flavour astrophysical diffuse neutrino flux were derived from data of NT200 neutrino telescope [3, 4]. Demonstration cluster of the GVD is an array which have a potential for study the flux of astrophysical neutrinos at a level obtained by IceCube. Neutrino effective areas for each flavor assuming an equalflux of neutrinos and antineutrinos and averaged over all arrival angles are shown in figure 11 (left panel). These areas are about of factor 10 less than relative areas of IceCube. The accuracy of a shower direction reconstruction is about of 4 degree (median value), which is substantially better than 10 degree accuracy for the IceCube. The fraction of shower events (Esh = 100 TeV) with mismatch angles between generated and reconstructed muon directions less than a given value ψ is shown in figure 11 (right). Energy distrfibutions of expected shower events per year from IceCube astrophysical fluxes for different flavours and all-flavour flux, as well as distribution of expected background

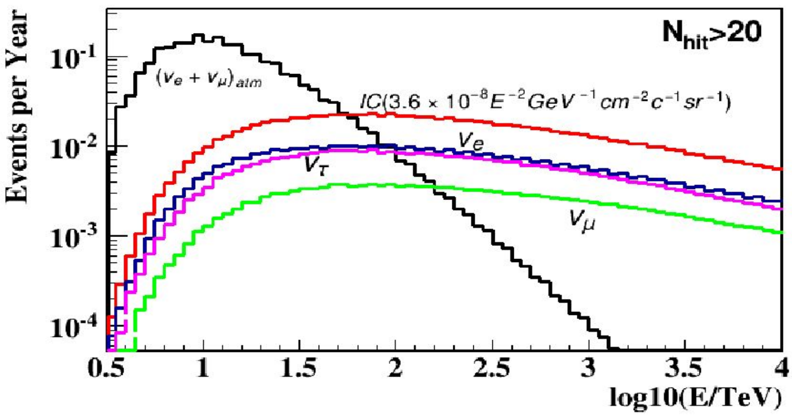

Figure 12: Expected distributions of events from astrophysical fluxes obtained by IceCube per year. Also shown is a distribution of background events from atmospheric neutrinos.

shower events from atmospheric neutrinos are shown in figure 12. About one event per year with shower energy more than 100 TeV from astrophysical flux is expected, to 10 events in IceCube.

The first stage of demonstration cluster “DUBNA”

In April 2011 the first autonomous engineering array which includes preproduction modules of all elements, measuring and communication systems, as well as prototype of acoustic positioning system of GVD-cluster has been installed and commissioned in Lake Baikal [14, 31].Array was connected to shore by electro-optical cable which was deployed also in 2011. In April 2012 the next version of engineering array which comprises 36 OMs has been deployed in Lake Baikal [32]. This array consists of two short strings and the first full-scale string of the GVD demonstration cluster “DUBNA” with 24 OMs.

The next important step on realization of the GVD project was made in 2013 and 2014 by

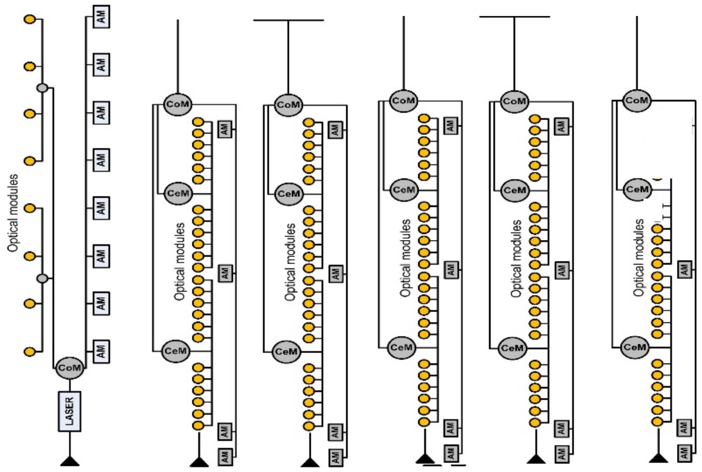

Figure 13: Schematic drawing of the 2014 year engineering array.

deployment of enlarged engineering array - the first stage of the demonstration cluster, which comprises 112 OMs arranged on three 345 m long strings, as well as instrumentation string with an array calibration and environment monitoring equipment [33]. The schematic view of this array is shown in figure 13. The vertical spacing of OMs is 15 m and the horizontal distance between strings is about of 40 m. In addition to OMs each string comprises the communication module (CoM), and two central modules of the sections. Also each string comprises one transmitter and 3 receivers of acoustic positioning system (AM) [34]. The modified cluster DAQ-center is located at separate cable station and is connected to shore by electrooptical cable. Instrumentation string is located at about of 100 m apart from the measuring strings with OMs. It comprises the calibration laser source, eight optical modules, as well as 10 acoustic sensors of positioning system. The calibration laser source [35] is located at 1215 m depth and is used for time synchronization between OMs on different strings. High intensity of laser source (up to 6 x 10^{13} photons/pulse) allows illumination of OMs at distances more than 200 m from the source. Acoustic sensors are arranged along the instrumentation string starting from the 50 m depth to the bottom of string and perform monitoring of the string displacements at different depths caused by deep or/and surface water currents. Eight optical modules housing R8055 or XP1807 PMTs are arranged at the depths from 600 m to 900 m on the instrumentation string and aim at monitoring of the light background at these depths.

The first stage of demonstration cluster was successfully operated from April 2013 to up to now in several testing and data taking modes. Total of 5.5 x 10^7 events have been recorded for 2013 season, which relate to 216 days of lifetime. Figure 14 (left) gives an indication of the data taking efficiency during 2013. Shown in figure 14 (right) is a time difference between two consecutive events of data sample. An exponential behavior of this distribution is consistent with expectation for randomly distributed experimental events and illustrates quality of data. Long-term control and monitoring of the array measuring system behavior, as well as background conditions during array operation in 2013 have been performed. In figure 15 the PMTs counting rates in 2012 (left) and 2013 (right) are shown. The main contribution to recorded counting rates is made by radiation

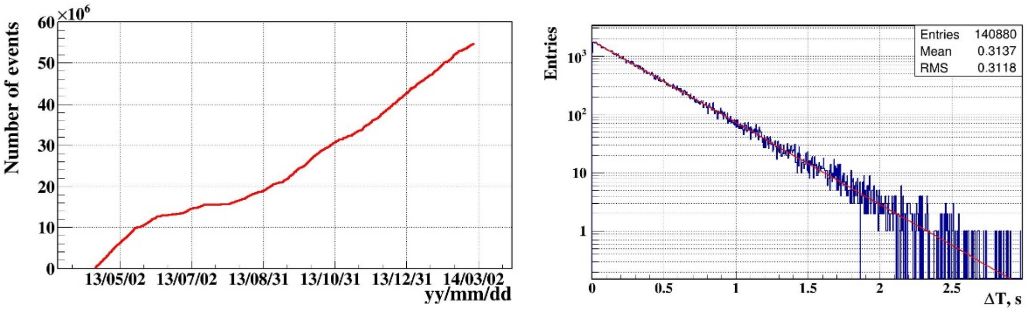

Figure 14: Left: Integrated number of recorded events in 2013 season. Right: Time difference between two consecutive events.

produced by chemiluminescence in the deep water. During April-August 2013 the PMTs counting rates are about of 10-20 kHz, which are comparable with values obtained in 2012. In August-September 2013 the rise of counting rates were indicated at different depths.

The counting rates behavior in this period is consistent with the movement of approximately 200 m thick layer of water with high level of background light from top to bottom with 6-7 m/day velocity.

One of the main goals of array operation in testing modes was an estimation of the ability of in-situ calibration procedures. Calibration of the array recording system consists of charge and timing calibrations of the measuring channels and time synchronization of OMs on different

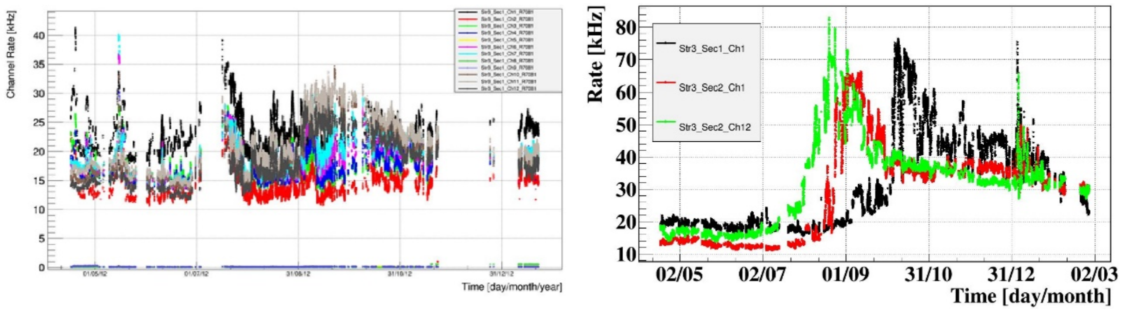

Figure 15: Left: Counting rates of OMs belonging to the bottom section of third string, which were observed in 2012. Right: Counting rates of OMs 1, 13 and 24 belonging to the third string, which were observed in 2013.

sections. All these calibration procedures are based on usage of OM's internal calibration LEDs and external laser light source.

The charge calibration enables to translate the signal amplitudes into number of photo-electrons (p.e.), which is the relevant information for muon and shower energy reconstruction. For charge calibration of PMTs a standard procedure based on an analysis of a single photoelectron spectrum (s.p.e.) has been applied. In this calibration mode the pulses of two

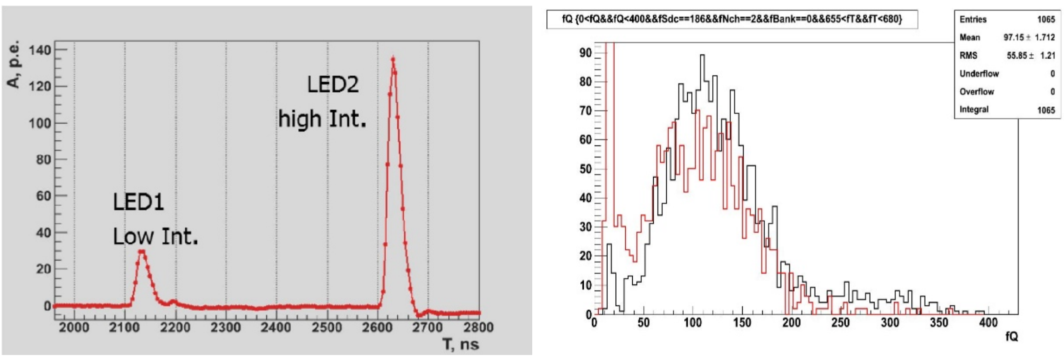

Figure 16: Left: Illustration of s.p.e. signal selection procedure. Right: Charge distributions of s.p.e. signals obtained by LEDs (top curve) and noise

LEDs of OM are used. Intensity of the first LED is fitted to provide a detection of s.p.e. signals with detection probability about of 10%. These pulses are used to measure s.p.e. distribution of channel signals. Pulses of the second LED with intensities corresponding to about of 50 p.e. of PMT's signal are delayed on 500 ns and are used as a trigger to suppress background signals with small amplitudes initiated by PMT dark current, as well as light background of the lake deep water. Figure 16 (left) illustrates this procedure. An optical activity from chemiluminescence of deep Lake Baikal water produces single photons at the photocathode level. Alternate procedure of charge calibration uses these noise events to study the single photo-electron peak. In figure 16 (right) charge distributions of s.p.e. signals of one of the PMTs obtained by LEDs (top curve) and noise analysis are shown.

The time calibration of measuring channels aims at control the relative offsets in times between PMTs, which are formed by PMTs internal delay and delay caused by signal passing through about of 90 m long cable connecting OM and CeM. Cable delays are measured once in the

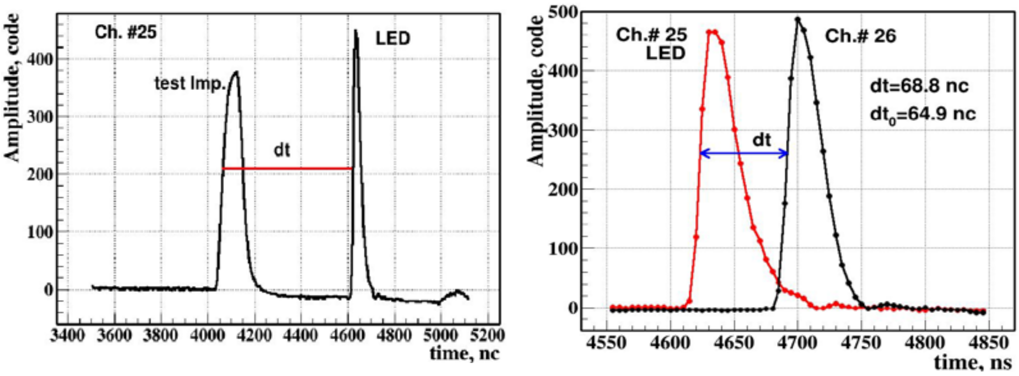

Figure 17: Left: Time distributions of the LED and reference signals that are used for measurement of the PMT intrinsic delay. Right: Signals of PMT #25 and PMT #26 caused by LED located in OM #25. Expected time difference dt_0 = 64.9 ns and detected one dt= 64.9 ns, the relative offset is equal to 3.9 ns.

laboratory and are the same during array operation. PMT delay depends on a power voltage and thus it requires regular calibration during array operation. There is a reference pulse which is generated by OM controller and is delivered to point of signal generation in PMT preamplifier. Reference pulse initiation is synchronized with start time of LED. From measured difference between arrival times of LED signal and reference pulse the PMT delay is obtained. Figure 17 (left) illustrates this procedure.

Intensities of LEDs light bursts are high enough to illuminate neighboring PMTs on the string. It allows synchronization between OMs of different sections, as well as measurement of relative time offsets between channels inside one section. The time synchronization of different sections were performed and relative offsets between PMTs were derived by means of LEDs using a known locations of strings and OMs obtained from analysis of data accumulated by acoustic positioning system. Figure 17 (right) illustrates the time calibration of two neighboring PMTs by means of LED, located in one of them.

The performance and quality of using calibration procedures have been verified by reconstruction of position and intensity of the calibration laser source. An external calibration laser provides five series of 480 nm light pulses at five fixed intensity levels ranging from approximately 10^{12} to 6 x 10^{13} photons/pulse [12], which corresponds to shower energies from 10 PeV to 600 PeV. This allows to test the array ability for high-energy cascades detection and reconstruction. Location of the laser source was reconstructed using arrival times of photons detected by PMTs, taking into account the timing calibration of PMTs. Results of reconstruction were compared with the laser coordinates obtained by acoustic positioning

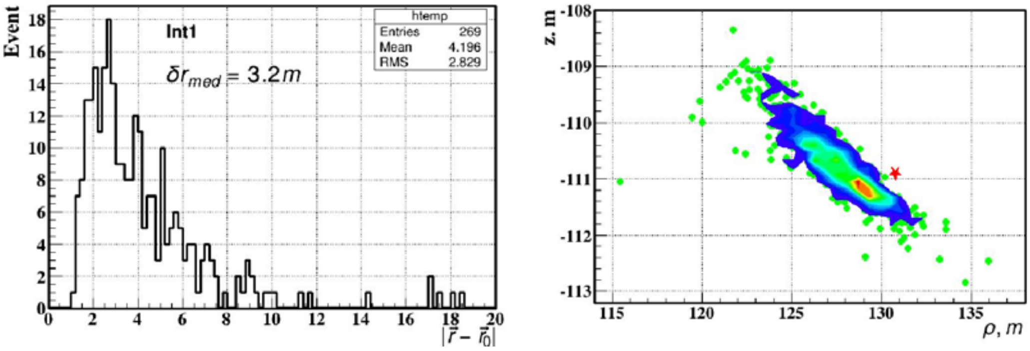

Figure 18: Left: Deviation of reconstructed laser coordinates from those obtained by acoustic positioning system. Right: Reconstructed laser positions on (p, z)- coordinates plane. Here *z* - vertical coordinate, *p* - horizontal distance from second string. Star indicates laser location obtained by acoustic positioning system.

system. Differences between reconstructed coordinates and those obtained by acoustic positioning system are shown in figure 18 (left). Reconstruction accuracy (median value) is about of 3 m. Shown in figure 18 (right) are reconstructed laser positions on (p, z)-coordinates plane. Here z is a vertical coordinate, p - horizontal distance from second string and star indicates the laser location obtained by acoustic positioning system.

Reconstruction of laser intensities were performed by using calibrated amplitudes of hit PMTs and taking into account a reconstructed position of laser source. Reconstructed intensities of four different series of laser bursts are shown in figure 19 (left). Relative uncertainty of intensity

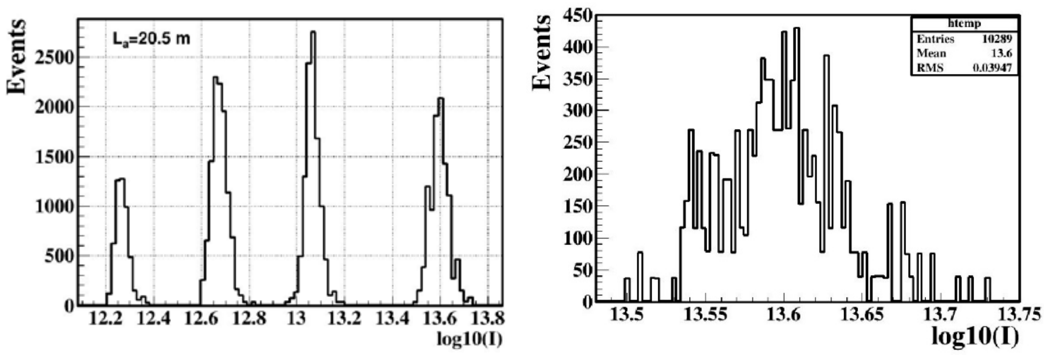

Figure 19: Left: Reconstructed intensities of four series. Right: Reconstructed intensities for the most intensive series of laser bursts.

reconstruction is less than 10% (see figure 19 (right)). Obtained results of reconstruction of position and intensity of the laser source proves an expected quality of array calibration procedures. Deployment of the demonstration cluster will be completed in 2015.

Results for last 3 years

- Most important result is deploying . In April 2012 the next version of engineering array which comprises 36 OMs has been deployed in Lake Baikal [32]. This array consists of two short strings and the first full-scale string of the GVD demonstration cluster "DUBNA" with 24 OMs.The next important step on realization of the GVD project was made in 2013 and 2014 by deployment of enlarged engineering array - the first stage of the demonstration cluster, which comprises 112 OMs arranged on three 345 m long strings, as well as instrumentation string with an array calibration and environment monitoring equipment and is presently taking data. The demonstration cluster "DUBNA" will be completed in 2015 with 8 strings, comprising 196 optical modules.

- Primary analysis on data from the cluster was prepared. It shows expected performance of all part of the detector.

- New analysis of NT200 data for period 1998-2003 was prepared for search to neutrinos from dark matter annihilations in the Sun. Upper limits on the muon and neutrino fluxes, the annihilation rate and on the SD/SI cross sections of DM scattering on protons assuming different annihilation channels was derived. It was found that for DM masses below 500 GeV the best sensitivity is obtained for the annihilation in neutrino-antineutrino pairs.

- Papers has been published [1-11], talks [12-20] given at conferences (see List of publications and conferences).

Plans and future

Prototyping Phase of project will conclude in 2015 with deployment in Lake Baikal of the ANTARES-scale array – the first cluster "DUBNA" of BAIKAL-GVD.

In period 2016-2018 we are going to deploy 4 additional clusters. Thus, at the end of 2018 5 full clusters with 1440 OMs will be in operation. Thereforewe obtain the following effective volumes for showers with energies > 100 TeV: 2016 – 0.06 km^3; 2017 - 0.12; 2018 - 0.24km^3. That allows us to have about 10 events "IceCube" events

with energies > 100 TeV at the end of 2018 year.

Contribution of JINR Members

JINR Members are playing significant roles in all key parts of the BAIKAL experiment:

- Assembly and test of deep water components.
- Continuous monitoring of the detector operation and remote control.
- Development of on-line and off-line software for the experiment.
- Development of databases, data acquisition software.
- Detector calibration and mass processing of data.
- Monte Carlo simulation and creation of the data bank.
- Development of new methods of event selection and reconstruction.
- Data analysis with respect to extraterrestrial high energy neutrinos and neutrinos from dark matter annihilation.

List of publications and conferences

[1] A. Avrorin et al. “A Hydroacoustic Positioning System for the Experimental Cluster of the Cubic-Kilometer-Scale Neutrino Telescope at Lake Baikal”. In: *Instruments and Experimental Techniques* 56.4 (2013), p. 449.

[2] A. Avrorin et al. “The Baikal neutrino experiment”. In: *Nucl. Instr. and Meth., A* 626 (2011), p. 13.

[3] A. Avrorin et al. “The Baikal neutrino project: Present and Perspectives”. In: *Nucl. Instr. and Meth., A* 628 (2011), p. 115.

[4] A. Avrorin et al. “The Baikal neutrino telescope - Results and plans”. In: *Nucl. Instr. and Meth., A* 630 (2011), p. 115.

[5] A. Avrorin et al. “The Gigaton Volume Detector in Lake Baikal”. In: *Nucl. Instr. and Meth., A* 639 (2011), p. 30.

[6] A. Avrorin et al. “Status of the BAIKAL neutrino experiment”. In: *Bulletin of the Russian Academy of Sciences. Physics* 75.3 (2011), p. 414.

[7] A. Avrorin et al. “Search for neutrino events from Gamma Ray Bursts in NT200”. In: *Lett. To Astron. J.* 37.10 (2011), p. 1.

[8] A. Avrorin et al. “Acoustic search for high-energy neutrinos in the Lake Baikal: Results and plans.” In: *Nucl. Instr. and Meth., A* 662 (2012), p. 210.

[9] A. Avrorin et al. “Status of the BAIKAL-GVD project”. In: *Nucl. Instr. and Meth., A* 692 (2012), p. 46.

[10] A. Avrorin et al. “ASP-15 - A stationary device for the measurement of the optical water

properties at the NT200 neutrino telescope site". In: *Nucl. Instr. and Meth., A* 693 (2012), p. 186.

[11] A. Avrorin et al. "Current status of the BAIKAL-GVD project". In: *Nucl. Instr. and Meth., A* 725 (2013), p. 23.

[12] A. Avrorin et al. "Present status of the BAIKAL-GVD project development". In: *Journal of Physics:Conference Series* 409 (2013), p. 012141.

[13] Zh.-M.Dzhilkibaev. In: 3rd Roma International Conference on Astro-particle Physics (RICAP 2011), Rome. 2011.

[14] V.Aynutdinov. In: 2nd International Cosmic Ray Conference (ICRC-2011), Beijing, China. 2011.

[15] Zh.-M.Dzhilkibaev. In: Mediterranean and Antarctic Neutrino Telescope Symposium (MANTS), Bologna, Italy. 2011.

[16] I.Belolaptikov. In: 23rd European Cosmic Ray Symposium, Moscow, Russia. 2012.

[17] B. Shoybonov. In: The XXV International Conference on Neutrino Physics and Astrophysics, Kyoto, Japan. 2012.

[18] N.Budnev. "Status of the BAIKAL-GVD neutrino project". In: International Cosmic Ray Conference (ICRC-2013), Rio de Janeiro, Brazil. 2013.

[19] Zh.Dzhilkibaev. "The prototyping/early construction phase of the BAIKAL-GVD project". In: Roma International Conference on AstroParticle Physics (RICAP-13), Rome, Italy. 2013.

[20] O. Suvorova. "Search for Neutrinos from Dark Matter Annihilation in the Sun with the Baikal Neutrino Experiment". In: Workshop EPNT13: "Exotic Physics with Neutrino Telescopes 2013", Marseille, France. 2013.

References

[1] BAIKAL Collaboration. *BAIKAL - GVD.* Tech. rep. Gigaton Volume Detector in Lake Baikal(Scientific-Technical Report). 2011. URL: http://baikalweb.jinr.ru/gvd/BAIKAL-GVD_En.pdf.

[2] *A.Avrorin et al.* // Nucl. Instr. and Meth. A. 2012. V.693 P.186.

[3] *V.Aynutdinov et al.* // Astropart. Phys. 2006. V.25 P.140.

[4] *A.Avrorin et al.* // Astronomy Lett. 2009. V.35 P.651.

[5] *I.A. Belolaptikov, et al.* // Astropart. Phys. 1997. V.7 P.263.

[6] *V.M. Aynutdinov, et al.* // Astropart. Phys. 2008. V.29 P.366.

[7] *A.V. Avrorin, et al.* // Astronomy Lett. 2011. V.37 P.692.

[8] *V. Aynutdinov et al.* // Nucl. Instr. and Meth. A. 2009. V.602 P.227.

[9] *A. Avrorin et al.* // Nucl.Instr. andMeth. A. 2011.V.626 S13.

[10] *A. Avrorin et al.* // Nucl.Instr. andMeth. A. 2011.V.630 P.115.

[11] *A. Avrorin et al.* // Nucl.Instr. andMeth. A. 2011.V.639 P.30.

[12] *A.V. Avrorin et al.* // Instr. and Exp. Tech. 2011. V.54 P.649.

[13] *A. Avrorin et al.* // Nucl.Instr. andMeth. A. 2012.V.692 P.46.

[14] Y. Fukuda et al. "Evidence for oscillation of atmospheric neutrinos". In: *Phys. Rev. Lett.* 81 (1998), p. 1562.

[15] P.-A. M. Dirac. In: *Proc. Roy. Soc.* A133 (1931), p. 60.

[16] Frank I.M. *Vavilov-Cherenkov radiation.* Russian. Moscow: Nauka, 1988, p. 192.

[17] G. t'Hooft. In: *Nucl. Phys.:Proc. Suppl.* 79 (1974), p. 276.

[18] A. Polyakov. In: *JETP Lett.* 20 (1974), p. 194.

[19] Domogatskii G.V. and Zheleznykh I.M. In: *Sov. J. Nucl. Phys.* 10 (1969), p. 702.

[20] Parker E.N. In: *Astrophys. J.* 160 (1970), p. 383.

[21] Turner M.S. et al. In: *Phys. Rev.* D26 (1982), p. 1296.

[22] Rubakov V. A. In: *JETP Lett.* 33 (1981), p. 644.

[23] C. G. Callan. In: *Phys. Rev. D* 26 (1982), p. 2058.

[24] Bezrukov L. B. et al. In: *Sov. J. Nucl. Phys.* 52 (1990), p. 86.

[25] Berezinsky V. S. and Zatsepin G. T. Russian. In: *Sov. Phys.- Uspekhi* 122.1(500) (1977), pp. 1-36.

[26] J. Learned and K. Mannheim. "High-energy neutrino astrophysics". In: *Annu. Rev. Nucl. Part. Sci* 50 (2000), pp. 679-749.

[27] Katz U. and Spiering Ch. In: *Prog. Part. Nucl. Phys.* 67 (2012), p. 651.

[28] *M. G. Aartsen et al. [IceCube Collaboration]. // Science. 2013. V.342 1242856.*

[29] *M. G. Aartsen et al. [IceCube Collaboration].* // Phys. Rev. Lett. 2013. V.111, 021103.

[30] A. Avrorin et al. "A Hydroacoustic Positioning System for the Experimental Cluster of the Cubic-Kilometer-Scale Neutrino Telescope at Lake Baikal". In: *Instruments and Experimental Techniques* 56.4 (2013), p. 449.

[31] *A. Avrorin et al.* // Nucl.Instr. andMeth. A. 2013.V.725 P.23.

[32] *A. Avrorin et al.* // J. of Phys. Conf. Series. 2013. V.409 012141.

[33] *A.D. Avrorin et al.* // Nucl. Instr. and Meth. A. 2014. V.742 P.82.

[34] *A.V. Avrorin et al.* // Instr. and Exp. Tech. 2013. V.56 P.449.

[35] *A.V. Aynutdinov et al.* // Phys. of At. Nucl. 2006. V.69 P.1914.

Форма № 26

Предлагаемый план-график и необходимые ресурсы для осуществления проекта «БАЙКАЛ-GVD»

Наименование узлов и систем установки, ресурсов, источников финансирования			Стоимость узлов (.$) установки. Потребности в ресурсах	Предложения Лабораторий по распределению финансирования и ресурсов		
				1 год	2 год	3 год
Основные узлы и оборудование	2. Элементы глубоководного оптического модуля (ФЭУ, стеклосферы, электроника)		8430K	2810K	2810K	2810K
	3. Глубоководные разъемы		1800K	600K	600K	600K
	4. Элементы подводной электронной системы управления и сбора данных		1050K	350K	350K	350K
	5. Элементы подводных кабельных коммуникаций		600K	200K	200K	200K
	6. Элементы системы позиционирования		2100K	700K	700K	700K
	7. Транспортные ср-ва и развитие инфраструктуры (береговой центр, транспортер на воздушной подушке)		2400K	800K	800K	800K
	8. Оптоэлектрический кабель и средства развертывания		1200K	400K	400K	400K
	Итого		**17580K**	**5860K**	**5860K**	**5860K**
Необходимые ресурсы	**Нормо-часы**	ОП ОИЯИ	6000	2000	2000	2000
		ООЭП ЛЯП	3300	1100	1100	1100
Источники финансирования	Бюджет	**Затраты из бюджета**	**15000K**	**5000K**	**5000K**	**5000K**
	Внебюджетные средства	**Вклады коллаборантов.** Средства по грантам. Вклады спонсоров Средства по договорам. Другие источники **и т.д.**	**3000K**	**1000K**	**1000K**	**1000K**

Руководитель проекта **И.А.Белолаптиков**

Форма № 29

Смета затрат по проекту «БАЙКАЛ»

№№ пп	Наименование статей затрат	Полная стоимость	1 год	2 год	3 год
	Прямые затраты на Проект				
1.	Компьютерная связь	. 15.0K US$	5.0	5.0	5.0
2	ООЭП ЛЯП	3300 норм ч.	1100	1100	1100
3.	ОП ОИЯИ	6000 норма ч.	2000	2000	2000
4.	Материалы	12300.0K US$	4100.0	4100.0	4100.0
5.	Оборудование	5280.0K US$	1760.0	1760.0	1760.0
6.	Оплата НИР, выполняемых по договорам	30.0K US$	10.0	10.0	10.0
7.	Командировочные расходы	150.0K US$	50.0	50.0	50.0

Итого по прямым расходам	**17775.0K US$**	**5925.0K $**	**5925.0K $**	**5925.0K $**

Руководитель Проекта

Директор Лаборатории

Ведущий инженер-экономист
Лаборатории